



The impact of modifiable factors on image quality of prostate magnetic resonance imaging and PI-RADS scores

Lukas Lambert^{1^}, Iva Macova², Monika Wagnerova², Martin Jurka², Romana Burgetova^{2,3}, Otakar Capoun⁴, Andrea Burgetova²

¹Department of Imaging Methods, Second Faculty of Medicine, Charles University and Motol University Hospital, Prague, Czech Republic;

²Department of Radiology, First Faculty of Medicine, Charles University and General University Hospital in Prague, Prague, Czech Republic;

³Department of Radiology, Third Faculty of Medicine, Charles University, Prague, Czech Republic; ⁴Department of Urology, First Faculty of Medicine, Charles University and General University Hospital in Prague, Prague, Czech Republic

Contributions: (I) Conception and design: L Lambert, A Burgetova; (II) Administrative support: L Lambert; (III) Provision of study materials or patients: O Capoun; (IV) Collection and assembly of data: I Macova, M Wagnerova, M Jurka, R Burgetova, O Capoun; (V) Data analysis and interpretation: L Lambert; (VI) Manuscript writing: All authors; (VII) Final approval of manuscript: All authors.

Correspondence to: Prof. Lukas Lambert, MD, MSCS, PhD. Department of Imaging Methods, Second Faculty of Medicine, Charles University and Motol University Hospital, V Uvalu 84, 150 06 Prague 5, Czech Republic. Email: lambert.lukas@gmail.com.

Background: The diagnostic accuracy of prostate magnetic resonance imaging (MRI) is highly dependent on image quality. Although the effects of spasmolytics and rectal preparation have been previously studied, the findings remain inconsistent and fail to address other critical modifiable factors. This study aimed to evaluate the impact of various modifiable factors on prostate MRI image quality and their subsequent influence on Prostate Imaging Reporting and Data System (PI-RADS) scoring.

Methods: Fifty-six consecutive patients who underwent 3T multiparametric MRI (mpMRI) with the administration of hyoscine butylbromide (HB+) and at least one 3T mpMRI without HB (HB-) ≤ 3 years earlier were retrospectively evaluated. Two radiologists performed morphometry of the prostate, bladder, rectum, and abdomen and evaluated image quality, artifacts, and motion on a five-point scale and T2 and diffusion-weighted imaging (DWI) PI-RADS v2.1 scores. The influence of HB, rectum and bladder distension, breathing motion, and examination hour were analyzed.

Results: The sharpness and overall image quality of T2 images were significantly better in HB+ compared to HB- ($P=0.0047$ and $P=0.013$). T2 motion artifacts were reduced earlier in the day ($p=0.32$, $P=0.017$). DWI susceptibility artifact correlated with patient diameter ($p=0.40$, $P=0.002$), but not with rectum diameter ($p=0.09$, $P=0.51$) or gas content ($p=0.13$, $P=0.33$). Examinations later in the day were associated with increased motion artifacts on T2 [hazard ratio (HR) =1.36]. T2 and DWI scores were influenced by bladder volume, breathing motion, and rectal air, but not by HB. Breathing motion negatively impacted overall image quality (HR =1.24), and DWI susceptibility artifacts (HR =1.22).

Conclusions: HB administration, daytime, and breathing motion have significant influence on image quality of prostate MRI. The gas content of the rectum influences T2 image quality and T2 scores. Bladder filling is associated with reduced breathing motion, subsequently affecting DWI scores.

Keywords: Magnetic resonance imaging (MRI); prostate; cancer; Prostate Imaging Reporting and Data System (PI-RADS); hyoscine butylbromide (HB)

[^] ORCID: 0000-0003-2299-4707.

Submitted Aug 26, 2024. Accepted for publication Feb 07, 2025. Published online Feb 26, 2025.

doi: 10.21037/qims-24-1776

View this article at: <https://dx.doi.org/10.21037/qims-24-1776>

Introduction

Magnetic resonance imaging (MRI) of the prostate gland is a cost-effective tool for the detection of prostate cancer (1). The image quality of the multiparametric MRI (mpMRI) of the prostate influences its positive predictive value and the proportion of Prostate Imaging Reporting and Data System (PI-RADS) 3 findings (2).

Image quality on multiparametric MRI (mpMRI) is influenced by numerous factors that originate from the MRI scanner capabilities, MRI sequence parameters, and also from the patients themselves (3). Patient-related factors can be influenced by their management, preparation before the examination, and guidance. Patient preparation strategies that encroach on patients' well-being have been subject to substantial research with contradicting conclusions (4,5). Microenema preparation, laxatives, and insertion of rectal catheter are becoming less popular due to their uncertain benefit compared to added discomfort (4). The opinion on the use of spasmolytics such as hyoscine butylbromide (HB) or glucagon is divided but they are used in numerous centers (6-8). Their use may be reconsidered in bi-parametric MRI (bpMRI) of the prostate as they require additional intravenous or intramuscular injection (9,10). Other strategies including abdominal compression, patient guidance on breathing during the examination, the need for emptying before the examination, and fasting are researched to a lesser extent and their use is based on sharing individual experience. This raises the need to explore the modifiable factors together within a single study group.

This study aimed to quantify the influence of modifiable factors including motion of the abdominal wall and rectum, filling of the bladder and rectum, and the administration of HB on the image quality of mpMRI and PI-RADS scores. We present this article in accordance with the STROBE reporting checklist (available at <https://qims.amegroups.com/article/view/10.21037/qims-24-1776/rc>).

Methods

This retrospective study was carried out in agreement with the Declaration of Helsinki (as revised in 2013). The Ethics Committee of the General University Hospital in Prague stated that the study required neither its approval nor

informed consent (199/22 S-IV).

Patient population

In this study, we included consecutive patients, who underwent mpMRI for suspected or known prostate cancer with the administration of HB between June 01, 2021 and Apr 17, 2023 and had at least one mpMRI before June 01, 2021 without HB ≤ 3 years apart. Since June 01, 2021, intravenous (i.v.) injection of 20 mg HB has been introduced prior to the MRI scan unless there was a contraindication, refusal by the patient, or the patient intended to drive a car.

The inclusion criteria were: mpMRI examination with and without HB ≤ 3 years apart for suspected or known primary prostate cancer; age ≥ 45 years. The exclusion criteria were: prostatectomy, severe artifacts from metallic implants, and radial data acquisition on T2. The flow chart is presented in *Figure 1*.

Magnetic resonance (MR) acquisition

The examinations were performed on a 3T scanner, Magnetom Skyra (Siemens, Forchheim, Germany) using phased-array coils according to the European Society of Urogenital Radiology (ESUR) guidelines (11). The examination included true fast imaging with steady-state free precession (TRUFI) in the sagittal plane, T1 volume interpolated breath-hold examination (VIBE) in the transverse plane, small field-of-view T2 turbo-spin-echo (TSE), and 3D T2 space in the transverse plane (3D T2 space was replaced by coronal T2 TSE since 1/9/2020), diffusion-weighted imaging (DWI) including $b=1,600$ mm/s, and dynamic contrast enhancement (DCE) (T1 VIBE) with a temporal resolution of 8 s. The imaging sequences used are described in *Table 1*.

Before positioning the patient in the scanner, HB (20 mg, Buscopan, Boehringer, Ingelheim, Germany) was administered intravenously in the second examination approximately 2 minutes before the localizer.

MR evaluation and data processing

MRI studies were reviewed on a clinical workstation

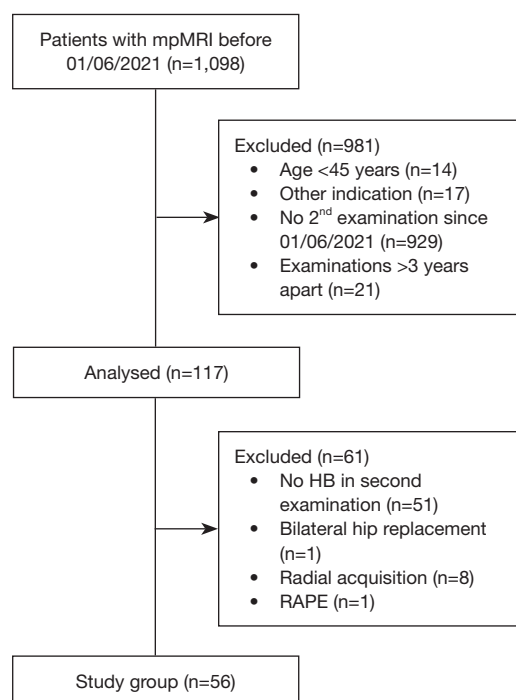


Figure 1 Study flowchart. HB, hyoscine butylbromide; RAPE, radical prostatectomy.

(Intellispace Portal, Philips, Best, Netherlands) by two radiologists with experience in reading prostate MR (11 and 4 years). Each radiologist, blinded to the administration of HB, evaluated MR examinations from half of the study group in a random order so that studies from one patient were separated by at least six other examinations. To assess interobserver agreement, each of the radiologists rated or scored MR images in additional 18 patients.

The measured parameters were:

- ❖ Body anteroposterior (AP) diameter on T1 images at the level of the prostate base;
- ❖ Maximum rectum internal AP diameter on T2 images at the level of the prostate base;
- ❖ The proportion of air content in the rectum was estimated at the same level;
- ❖ Bladder AP, lateral-lateral (LL), and caudocranial (CC) dimensions on T1 and TRUFI images with calculated volume for ellipsoid ($AP \times LL \times CC \times 0.52$);
- ❖ Prostate AP, LL, and CC dimensions on T2 and TRUFI images with calculated volume for ellipsoid ($AP \times LL \times CC \times 0.52$).

Table 1 Imaging sequence parameters

| Sequence name | TRUFI SAG | T1 VIBE TRA | T2 TSE TRA | T2 TSE COR [†] | 3D T2 SPACE [†] | DWI | T1 VIBE (DCE) |
|-----------------------------------|-----------|-------------|------------|-------------------------|--------------------------|-----------|---------------|
| Type | SSFP | T1 VIBE | 2D TSE | 2D TSE | 3D TSE | SS SE EPI | T1 VIBE |
| Image orientation | SAG | TRA | TRA | COR | TRA | TRA | TRA |
| FOV (freq × phase) (mm × mm) | 500×500 | 358×440 | 200×200 | 200×200 | 184×184 | 180×180 | 260×260 |
| Acquisition matrix (freq × phase) | 320×320 | 320×260 | 320×320 | 320×320 | 256×256 | 114×114 | 192×192 |
| TE (ms) | 1.65 | 1.2 | 101 | 101 | 104 | 67 | 1.8 |
| TR (ms) | 680 | 4.0 | 7,500 | 7,500 | 1,700 | 3,800 | 5.1 |
| Slice thickness (mm) | 5 | 3.0 | 3.5 | 3.5 | 1.0 | 3.5 | 3.5 |
| Slice gap (mm) | 1 | 0 | 0 | 0 | 0 | 0 | 0 |
| Slices | 30 | 72 | 26 | 26 | 80 | 60 | 22×20 |
| Averages | 1 | 1 | 3 | 3 | 1.4 | 3/5/9 | 1 |
| Phase/foldover direction | A-P | A-P | R-L | R-L | R-L | A-P | A-P |
| Echo-train-length | 1 | 2 | 25 | 25 | 60 | 50 | 1 |
| Bandwidth (Hz/px) | 1,200 | 1,040 | 200 | 200 | 610 | 1,566 | 260 |
| Acquisition time (min:s) | 0:20 | 0:35 | 4:39 | 4:39 | 5:59 | 4:39 | 22×8 s |

[†], 3D T2 SPACE was replaced by T2 TSE COR since 1/9/2020. 2D, two-dimensional; 3D, three-dimensional; A-P, antero-posterior; COR, coronal; DCE, dynamic contrast enhancement; DWI, diffusion-weighted imaging; FOV, field of view; freq, frequency; R-L, right-to-left; SAG, sagittal; SPACE, Sampling Perfection with Application optimized Contrasts using different flip angle Evolution; SSFP, steady-state free precession; SS SE EPI, single-shot spin-echo echo planar imaging; TE, time to echo; TR, repetition time; TRA, transverse; TRUFI, true fast imaging with steady-state free precession; TSE, turbo-spin-echo; VIBE, volume interpolated breath-hold examination.

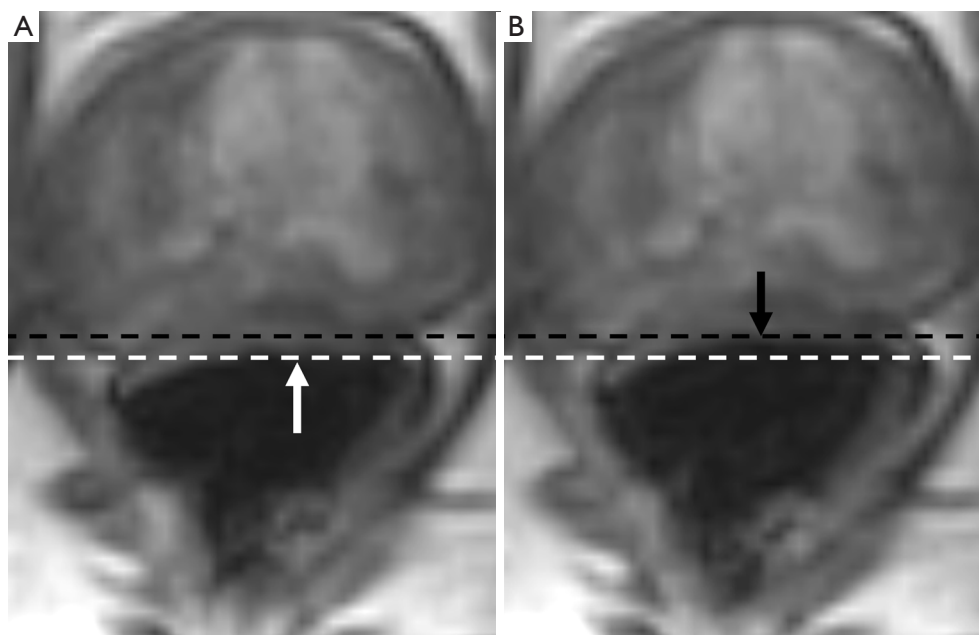


Figure 2 Anterior rectal wall motion evaluated on dynamic contrast enhancement MRI shows posterior (A) and anterior (B) excursions. Dashed lines and arrows indicate the outline of the posterior (A) and anterior (B) excursions. MRI, magnetic resonance imaging.

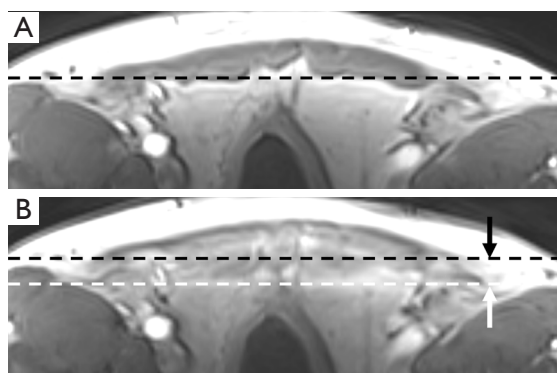


Figure 3 Abdominal wall respiratory motion evaluated on dynamic contrast enhancement MRI shows inspiratory (A) and expiratory (B) excursions. Dashed lines and arrows indicate the outline of the internal wall position in inspiration (A) and expiration (B). MRI, magnetic resonance imaging.

Further parameters were scored on 5-point Likert scales:

- ❖ Motion (1, none; 2, minimal; 3, mild; 4, moderate; 5, severe).
 - ♦ Motion of the anterior wall of the rectum (*Figure 2*, [Video S1](#));
 - ♦ Prostate motion on DCE;
 - ♦ Respiratory motion of the anterior abdominal

wall (*Figure 3*, [Video S1](#)).

- ❖ Artifacts (1, none; 2, mild; 3, moderate; 4, severe; 5, nondiagnostic) (12).
 - ♦ Motion artifacts on T2;
 - ♦ Susceptibility artifact on DWI.
- ❖ Image quality (1, excellent; 2, good; 3, moderate; 4, poor; 5, non-diagnostic) (13).
 - ♦ Overall image quality on T2.
- ❖ Anatomical resolution (1, excellent visualization: sharp delineation; 2, good delineation: slight blurring; 3, moderate visualization: moderate blurring; 4, poor visualization: heavily blurred appearance of structures; 5, non-diagnostic: structures cannot be evaluated) (13).
 - ♦ Anatomical detail (resolution) on T2 (*Figure 4*).
 - ♦ PI-RADSv2.1 score.
 - ♦ Maximum T2 score in transition zone.
 - ♦ Maximum DWI score in peripheral zone.

Statistical analysis

Statistical analysis was performed in R (R Foundation, Austria, Vienna), Prism (GraphPad Software, La Jolla, CA, USA), and SPSS (IBM Corp., Armonk, NY, USA). Pairwise comparisons were performed using the paired *t*-test or

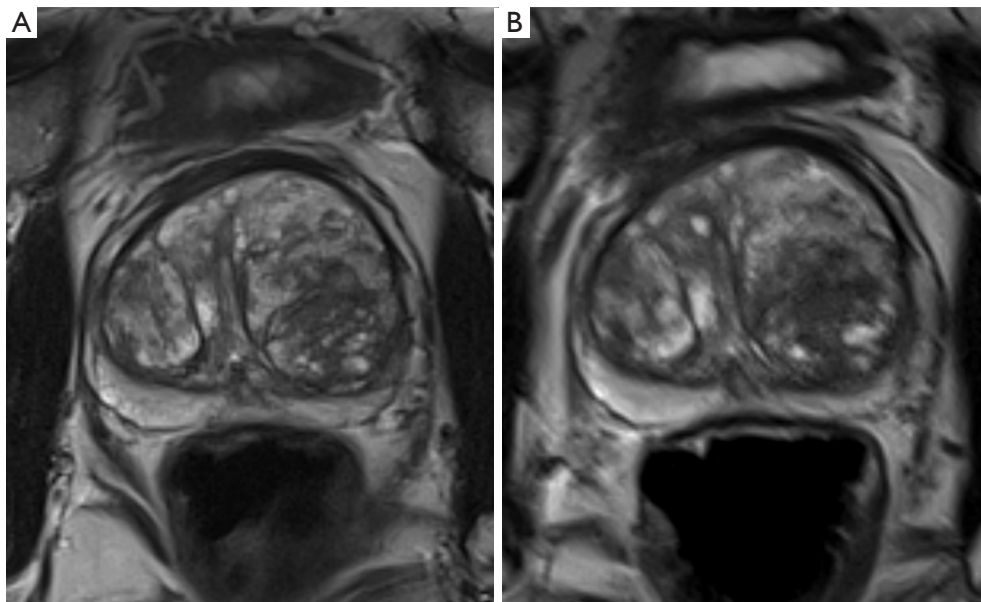


Figure 4 T2 images of the same patient demonstrate two levels of anatomical detail with sharp delineation of structures of the prostate gland (A) and heavily blurred image (B).

paired Wilcoxon test and expressed as mean \pm standard deviation or median [interquartile range (IQR)] according to their distribution (D'Agostino & Pearson omnibus normality test). Correlations were calculated using *rcorr* function for Spearman rank correlation (ρ , ρ).

The cross-correlation matrix was plotted using the *corrplot* function in R (unadjusted P values due to exploratory analysis). Interobserver agreement was calculated using *cohen.kappa* function (*psych package*) in R as weighted Cohen's kappa (κ). DWI and T2 PI-RADS scores of 1 and 2 were assumed as equal.

Linear regression model was constructed for all examinations and HB- examinations separately using values that can be influenced (the hour of the examination, rectum AP diameter, rectal air %, bladder volume, and breathing motion).

A P value <0.05 was considered significant. The minimum required sample size was calculated for a paired test with a significance of $\alpha=0.05$, power of $\beta=0.20$, and a medium effect size $E=0.5$ on 34 patients.

Results

Fifty-six patients (age, 66.5 ± 8.4 years; weight, 91.2 ± 15.6 kg) met the inclusion criteria and were finally evaluated (Figure 1). The second examination with HB was performed

21.8 ± 8.0 months after the examination without HB. The primary indication for the examination was elevated or rising prostate-specific antigen (PSA) levels (\pm previous negative biopsy, $n=53$), and active surveillance ($n=3$).

Pairwise comparisons

The examination in HB+ patients was performed 43 minutes earlier than in HB- patients ($P=0.0029$). Morphological measurements showed no significant difference between HB- and HB+ examinations (Table 2).

The image sharpness of the T2 TSE on HB+ was rated better ($P=0.0047$) and so was the overall image quality ($P=0.013$). No significant difference was found in the respiratory motion of the abdominal wall, motion of the anterior rectal wall on DCE, as well as in the motion or susceptibility artifacts, maximum T2 or DWI scores (Table 2). The interobserver agreement in rated items is shown in Table S1.

Cross-correlation

The cross-correlation exploratory analysis was performed for HB- examinations for selected parameters (Table 2, Figure 5). In HB- examinations, the T2 motion artifact was less pronounced in larger patients ($\rho=-0.36$, $P=0.006$)

Table 2 Patient's characteristics, measured, and estimated parameters from MRI

| Parameter | HB– | HB+ | P |
|---------------------------------------|---------------------|----------------------|----------|
| Age (years) | 66.5±8.4 | 68.3±8.3 | <0.0001* |
| Hour of examination (24 h) | 9.4±1.3 | 8.7±1.1 | 0.0029* |
| Body AP [†] (mm) | 224±30 | 224±32 | 0.87 |
| Rectum AP [†] (mm) | 33.2±11.6 | 32.8±11.8 | 0.85 |
| Air in rectum [†] (%) | 10 (5 to 20) | 8 (5 to 20) | 0.33 |
| Bladder AP [†] (mm) | 66.0±14.8 | 64.8±19.6 | 0.58 |
| Bladder LL (mm) | 68.6±14.2 | 64.7±14.8 | 0.013* |
| Bladder CC (mm) | 47.6±23.3 | 44.4±21.2 | 0.18 |
| Bladder volume [†] (mL) | 103 (61 to 140) | 100 (46 to 154) | 0.33 |
| Prostate volume [†] (mL) | 69.4 (53.3 to 98.8) | 70.2 (52.9 to 100.5) | 0.66 |
| Prostate AP (mm) | 44.9±7.3 | 45.0±8.5 | 0.82 |
| Prostate LL (mm) | 55.6±7.3 | 56.2±8.0 | 0.33 |
| Prostate CC (mm) | 56.5±9.3 | 55.9±9.0 | 0.45 |
| Rectal wall motion DCE [†] | 2.0 (1.0 to 2.0) | 2.0 (1.0 to 2.0) | 0.95 |
| Prostate motion DCE [†] | 1.0 (1.0 to 2.0) | 1.0 (1.0 to 2.0) | 0.66 |
| Breathing motion DCE [†] | 2.0 (2.0 to 3.0) | 2.0 (2.0 to 3.0) | 0.55 |
| Anatomical resolution T2 [†] | 2.0 (1.0 to 2.8) | 1.0 (1.0 to 2.0) | 0.0047* |
| Motion artifacts T2 [†] | 1.0 (1.0 to 2.0) | 1.0 (1.0 to 2.0) | 0.082 |
| Overall quality T2 [†] | 2.0 (1.0 to 2.0) | 1.0 (1.0 to 2.0) | 0.013* |
| Susc. artifact DWI [†] | 1.0 (1.0 to 2.0) | 2.0 (1.0 to 2.0) | 0.24 |
| Max T2 score | 2.0 (2.0 to 2.0) | 2.0 (2.0 to 2.0) | 0.20 |
| Max DWI score | 2.0 (1.0 to 2.0) | 2.0 (1.0 to 2.0) | 0.13 |

Numbers are presented as mean ± standard deviation or median (IQR). [†], parameters used in cross-correlation analysis; *, P values <0.05. AP, anteroposterior; CC, caudocranial; DCE, dynamic contrast-enhancement imaging; DWI, diffusion-weighted images; HB, hyoscine butylbromide; HB–, examinations without HB; HB+, examinations with HB; IQR, interquartile range; LL, laterolateral; MRI, magnetic resonance imaging; susc., susceptibility; T2, T2-weighted images.

at an earlier hour ($\rho=0.32$, $P=0.017$). T2 resolution was impaired by rectal ($\rho=0.27$, $P=0.046$) and prostate motion ($\rho=0.31$, $P=0.018$). Higher rectal air content correlated with improved T2 overall image quality ($\rho=-0.28$, $P=0.038$). The DWI susceptibility artifact correlated with the AP diameter of the patient ($\rho=0.40$, $P=0.002$), but not with the rectum diameter ($\rho=0.09$, $P=0.51$, [Figure S1](#)) or gas content ($\rho=0.13$, $P=0.33$).

Linear regression

The best predictor of resolution and motion of T2 images was the hour of the examination [hazard ratio (HR) =1.34

and HR =1.36, respectively]. HB entered a linear regression model for T2 resolution (HR =0.82) and overall T2 image quality (HR =0.80, [Table 3](#)). Breathing motion deteriorated T2 resolution (HR =1.21), overall image quality (HR =1.24), and DWI susceptibility artifacts (HR =1.22). A greater amount of rectal air improved overall T2 image quality (HR =0.76). The T2 and DWI scores were influenced by the bladder volume, breathing motion, and rectal air, but not HB ([Table 4](#)).

Discussion

In this study, we showed that T2 image quality and motion

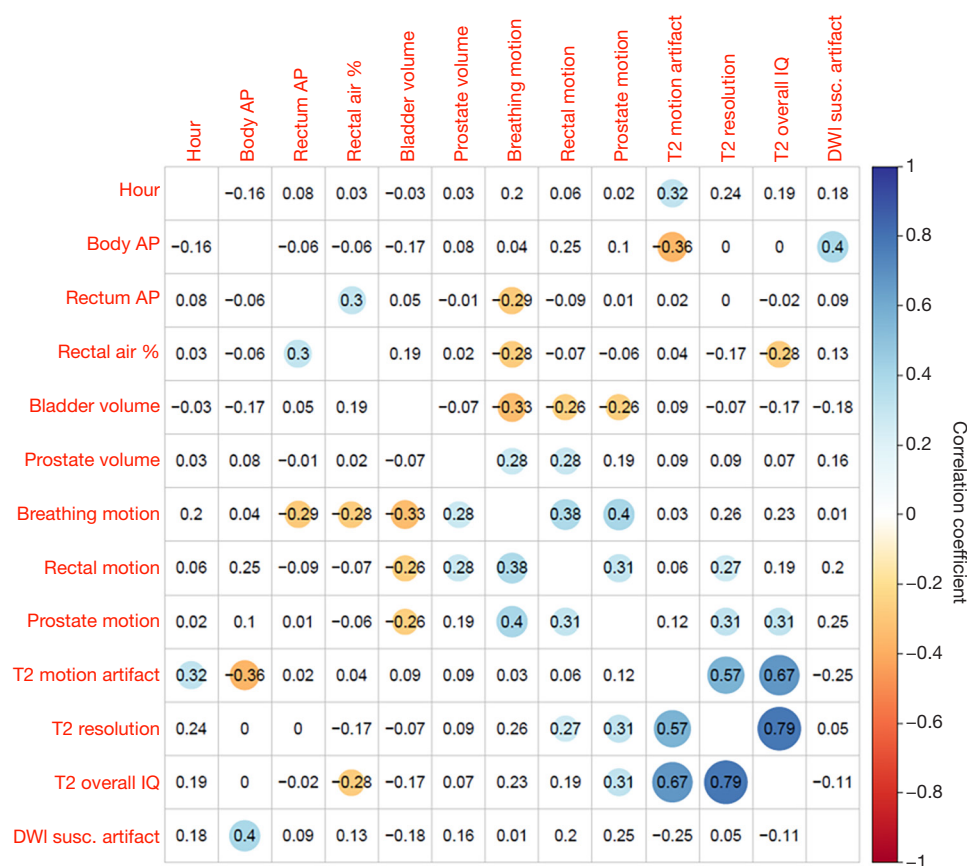


Figure 5 Cross-correlation plot for measured and estimated parameters on mpMRI without HB. Positive significant correlations are marked with blue color and negative with orange. Numbers represent Spearman's ρ rank correlation coefficients. AP, antero-posterior; DWI, diffusion-weighted imaging; HB, hyoscine butylbromide; IQ, image quality; mpMRI, multiparametric magnetic resonance imaging; susc., susceptibility; T2, T2-weighted imaging.

artifacts are influenced not only by HB injection but also by the daytime of the examination and breathing motion. The influence of the rectal distension is negligible. The T2 and DWI PI-RADS scores are influenced by bladder filling, breathing motion, and rectal air content, but not HB.

The quality of MRI with T2WI and DWI in the context of prostate imaging is influenced by numerous factors that reach beyond the technical specifications of the MRI scanner and the imaging parameters used. These include factors related to the management of the examination and patient preparation. There is no universally established, well-founded, evidence-based, efficacious, and generally accepted recommendation for preparing patients before MR examination of the prostate. Specific instructions supplied to the patient before and during the examination are based on expert group consensus and local experience (14). Preparations and recommendations to the patient before

MRI are put to a hypothetic scale where factors such as efficacy, cost, burden to the patient and personnel as well as examination time must be weighted (4).

Spasmolytics

Spasmolytics inhibit bowel peristalsis and reduce motion artifacts introduced by bowel peristalsis. Two drugs are commonly used. HB inhibits cholinergic ganglia of the visceral gut wall and shows antimuscarinic activity. It is cleared both for therapeutic and diagnostic use. Although it does not pass the hematoencephalic barrier, it has important contraindications including urine retention due to prostatic hyperplasia. Because HB impairs the accommodation of the eye lens, patients should be advised not to drive a car until normal vision is restored (8). The observed influence on peristalsis of intravenous HB is about 21 minutes (15).

Table 3 Linear regression models for image quality indicators for All and HB–

| Model [No.] | Variable entered | R ² | HR | Sig. |
|-----------------------------|-------------------|----------------|------|-------|
| T2 resolution | | | | |
| All [1] | Hour | 0.073 | 1.33 | 0.002 |
| All [2] | +Breathing motion | 0.101 | 1.21 | 0.001 |
| All [3] | +HB | 0.128 | 0.82 | 0 |
| HB– [1] | Hour | 0.055 | 1.34 | 0.045 |
| T2 motion | | | | |
| All [1] | Hour | 0.052 | 1.28 | 0.009 |
| HB– [1] | Hour | 0.078 | 1.36 | 0.021 |
| T2 overall image quality | | | | |
| All [1] | HB | 0.043 | 0.80 | 0.009 |
| All [2] | +Breathing motion | 0.081 | 1.24 | 0.004 |
| HB– [1] | Rectal air | 0.062 | 0.76 | 0.036 |
| DWI susceptibility artifact | | | | |
| All [1] | Breathing motion | 0.3 | 1.22 | 0.038 |
| HB– | No variables | – | – | – |

All, all examinations; DWI, diffusion-weighted imaging; HB, hyoscine butylbromide; HB–, examinations without hyoscine butylbromide; HR, hazard ratio; R², R-squared; Sig., significance; T2, T2-weighted images.

Glucagon is cleared for diagnostic procedures in the gastrointestinal tract (not the prostate) in adults and has a better safety profile with a rare occurrence of hypoglycemia. After intramuscular injection, the effect on peristalsis becomes apparent after 12 minutes and lasts 28 minutes (15). After diagnostic procedures, patients are required to refrain from driving unless they ingest carbohydrates to avoid hypoglycemia.

In previous studies, Schmidt *et al.* and Roethke *et al.* showed that HB did not demonstrate any effect on any subjective image quality measures (16,17), but others reported significant improvement of the anatomical T2W images and enhanced coherence of DCE and therefore advocated its use (6,7). In our study, the administration of HB improved anatomical resolution and overall image quality on T2 but did not influence DWI or T2 PI-RADS scores. The effect of HB was comparable to that of performing the examination at an earlier hour. This may be due to the peristalsis variation during the day (18). Patients may also be requested to avoid breakfast because the gastrocolic reflex is most active during the morning

Table 4 Linear regression models for T2 and DWI PI-RADS scores for All and HB–

| Model (No.) | Variable entered | R ² adj. | Beta std. | Sig. |
|-------------|-------------------|---------------------|-----------|-------|
| DWI score | | | | |
| All [1] | Bladder volume | 0.088 | 0.310 | 0.001 |
| All [2] | +Breathing motion | 0.148 | 0.304 | 0.000 |
| HB– [1] | Breathing motion | 0.108 | –0.353 | 0.008 |
| T2 score | | | | |
| All [1] | Rectal air % | 0.092 | 0.317 | 0.001 |
| HB– [1] | No variables | – | – | – |

All, all examinations; Beta std., standardized regression coefficient; DWI, diffusion-weighted images; HB, hyoscine butylbromide; HB–, examinations without hyoscine butylbromide; PI-RADS, Prostate Imaging Reporting and Data System; R² adj., adjusted R-squared; Sig., significance; T2, T2-weighted images.

time (19). The need for HB shall be reconsidered in patients undergoing bpMRI given the need for additional intravenous or intramuscular access.

Our findings demonstrate that time of day influences prostate MRI image quality, potentially contributing to variations in PI-RADS scores, as previously described by Becker *et al.* (20). While the ‘Hungry Judge’ effect proposed by Becker *et al.* suggests radiologist performance may be affected by circadian rhythms, our results suggest an additional mechanism: variations in image quality. Together, these findings underscore the importance of accounting for time-of-day effects in both image acquisition and interpretation processes.

Rectal preparation

Rectal distention has a negative effect on the quality of DWI and T2 (21). A positive effect of microenema on image quality and image artifacts has been shown in several studies (16,22). However, Coskun *et al.* showed that the effect of rectal microenema in a pairwise prospective study was only modest (23).

Padhani *et al.* showed that rectal distention correlated with rectal and prostate movements (24). In this study, we did not observe a direct correlation between rectal distension and the quality of the images obtained. Unexpectedly, the amount of rectal air improved the overall image quality on T2 images and also influenced T2 scores but had no impact on DWI susceptibility artifacts. This

discrepancy could point to the complex interplay of factors that influence MR image quality beyond rectal distension alone. Based on our results, we neither introduce rectal preparation nor ask patients to evacuate before prostate MRI.

Breathing instructions

No data are available about the effect of breathing instructions on image quality and diagnostic performance of prostate MRI. Dinkel *et al.* quantified prostate motion with respiration (25). During deep inspiration, the average displacement of the prostate was 2.7 ± 1.9 mm in the cardiocaudal axis and 1.8 ± 1.0 mm in the AP axis.

In our study, we showed that abdominal wall respiratory motion correlated with prostate motion and rectal wall motion on DCE, and it influenced T2 and DWI image quality and DWI PI-RADS scores. Our patients did not receive any specific instructions on breathing and did not have any mechanical restraints such as abdominal straps or sandbags.

These results show that the respiratory motion of the abdomen influences both the image quality and PI-RADS scores. We began to instruct patients to practice shallow chest breathing before and during the examination.

Bladder filling

In our study, bladder filling inversely correlated with breathing motion, and prostate motion, and influenced the DWI score. The effect of bladder filling on image quality was not significant. Previously, the effect of bladder volume on image quality on prostate MRI has not been investigated. In patients with full bladder, the respiratory wave in the abdomen is attenuated and bowel loops are displaced away from the prostate.

Image quality is not only necessary for efficient detection of prostate cancer, improved inter-reader variability, but it is also a prerequisite for image optimization using artificial intelligence and also for automated lesion detection and characterization, extraction of complex features from DWI, DCE, and novel imaging sequences such as amide proton transfer imaging (3,4,26-31).

Study limitations

Firstly, as this is a retrospective study, the strength of the associations being examined may be influenced by each other. Apart from HB, other factors that were evaluated

were not directly stratified. Second, the time between HB- and HB+ MRI is another confounding factor. Third, the subjective assessment of image quality has substantial limitations and introduces inherent biases and variability in the evaluation process, but this method has previously been used and was recognized. Fourth, the influence of the variables on depiction of extraprostatic findings has not been researched (32).

Conclusions

This study showed the influence of modifiable factors on the image quality of T2 and DWI images in prostate MRI. Apart from HB, other modifiable factors such as daytime and breathing motion have significant influence on image quality of prostate MRI. The gas content of the rectum influences T2 image quality and T2 scores. Bladder filling is associated with reduced breathing motion, subsequently affecting DWI scores. A multicenter study is warranted to explore interplay of these factors to a greater extent and support higher-level evidence-based recommendations.

Acknowledgments

We thank Miroslav Kron from the Department of Radiology, First Faculty of Medicine, Charles University and General University Hospital in Prague for technical assistance in data retrieval.

Footnote

Reporting Checklist: The authors have completed the STROBE reporting checklist. Available at <https://qims.amegroups.com/article/view/10.21037/qims-24-1776/rc>

Funding: This study was supported by the Ministry of Health of the Czech Republic (MH CZ-DRO, Motol University Hospital) (No. 00064203) and the Ministry of Health of the Czech Republic (General University Hospital in Prague) (No. 00064165) and the institutional funding of the Charles University in Prague (Cooperatio, Medical Diagnostics and Basic Medical Sciences) (UNCE 24/MED/018).

Conflicts of Interest: All authors have completed the ICMJE uniform disclosure form (available at <https://qims.amegroups.com/article/view/10.21037/qims-24-1776/coif>). L.L. serves as an unpaid editorial board member of

Quantitative Imaging in Medicine and Surgery. All authors report funding from the Ministry of Health of the Czech Republic (MH CZ-DRO, Motol University Hospital, No. 00064203 and General University Hospital in Prague, No. 00064165) and the institutional funding of the Charles University in Prague (Cooperatio, Medical Diagnostics and Basic Medical Sciences, UNCE 24/MED/018). The authors have no other conflicts of interest to declare.

Ethical Statement: The authors are accountable for all aspects of the work in ensuring that questions related to the accuracy or integrity of any part of the work are appropriately investigated and resolved. The study was conducted in accordance with the Declaration of Helsinki (as revised in 2013). The study was reviewed by the Ethics Committee of the General University Hospital in Prague that stated that the study required neither its approval nor informed consent (199/22 S-IV).

Open Access Statement: This is an Open Access article distributed in accordance with the Creative Commons Attribution-NonCommercial-NoDerivs 4.0 International License (CC BY-NC-ND 4.0), which permits the non-commercial replication and distribution of the article with the strict proviso that no changes or edits are made and the original work is properly cited (including links to both the formal publication through the relevant DOI and the license). See: <https://creativecommons.org/licenses/by-nc-nd/4.0/>.

References

- Hao S, Discacciati A, Eklund M, Heintz E, Östensson E, Elfström KM, Clements MS, Nordström T. Cost-effectiveness of Prostate Cancer Screening Using Magnetic Resonance Imaging or Standard Biopsy Based on the STHLM3-MRI Study. *JAMA Oncol* 2022;9:88-94.
- Brembilla G, Lavallo S, Parry T, Cosenza M, Russo T, Mazzone E, Pellegrino F, Stabile A, Gandaglia G, Briganti A, Montorsi F, Esposito A, De Cobelli F. Impact of prostate imaging quality (PI-QUAL) score on the detection of clinically significant prostate cancer at biopsy. *Eur J Radiol* 2023;164:110849.
- Jurka M, Macova I, Wagnerova M, Capoun O, Jakubicek R, Ourednicek P, Lambert L, Burgetova A. Deep-learning-based reconstruction of T2-weighted magnetic resonance imaging of the prostate accelerated by compressed sensing provides improved image quality at half the acquisition time. *Quant Imaging Med Surg* 2024;14:3534-43.
- Lin Y, Yilmaz EC, Belue MJ, Turkbey B. Prostate MRI and image Quality: It is time to take stock. *Eur J Radiol* 2023;161:110757.
- Prabhakar S, Schieda N. Patient preparation for prostate MRI: A scoping review. *Eur J Radiol* 2023;162:110758.
- Ullrich T, Quentin M, Schmaltz AK, Arsov C, Rubbert C, Blondin D, Rabenalt R, Albers P, Antoch G, Schimmöller L. Hyoscine butylbromide significantly decreases motion artefacts and allows better delineation of anatomic structures in mp-MRI of the prostate. *Eur Radiol* 2018;28:17-23.
- Slough RA, Caglic I, Hansen NL, Patterson AJ, Barrett T. Effect of hyoscine butylbromide on prostate multiparametric MRI anatomical and functional image quality. *Clin Radiol* 2018;73:216.e9-216.e14.
- Dyde R, Chapman AH, Gale R, Mackintosh A, Tolan DJ. Precautions to be taken by radiologists and radiographers when prescribing hyoscine-N-butylbromide. *Clin Radiol* 2008;63:739-43.
- Belue MJ, Yilmaz EC, Daryanani A, Turkbey B. Current Status of Biparametric MRI in Prostate Cancer Diagnosis: Literature Analysis. *Life (Basel)* 2022;12:804.
- Wang Y, Wang W, Yi N, Jiang L, Yin X, Zhou W, Wang L. Detection of intermediate- and high-risk prostate cancer with biparametric magnetic resonance imaging: a systematic review and meta-analysis. *Quant Imaging Med Surg* 2023;13:2791-806.
- Barentsz JO, Richenberg J, Clements R, Choyke P, Verma S, Villeirs G, Rouviere O, Logager V, Fütterer JJ; European Society of Urogenital Radiology. ESUR prostate MR guidelines 2012. *Eur Radiol* 2012;22:746-57.
- Sundaram KM, Rosenberg J, Syed AB, Chang ST, Loening AM. Assessment of T2-weighted Image Quality at Prostate MRI in Patients with and Those without Intramuscular Injection of Glucagon. *Radiol Imaging Cancer* 2023;5:e220070.
- Wagner M, Rief M, Busch J, Scheurig C, Taupitz M, Hamm B, Franiel T. Effect of butylscopolamine on image quality in MRI of the prostate. *Clin Radiol* 2010;65:460-4.
- Chang SD, Reinhold C, Kirkpatrick IDC, Clarke SE, Schieda N, Hurrell C, Cool DW, Tunis AS, Alabousi A, Diederichs BJ, Haider MA. Canadian Association of Radiologists Prostate MRI White Paper. *Can Assoc Radiol J* 2022;73:626-38.
- Gutzeit A, Binkert CA, Koh DM, Hergan K, von Weymarn C, Graf N, Patak MA, Roos JE, Horstmann

- M, Kos S, Hungerbühler S, Froehlich JM. Evaluation of the anti-peristaltic effect of glucagon and hyoscine on the small bowel: comparison of intravenous and intramuscular drug administration. *Eur Radiol* 2012;22:1186-94.
16. Schmidt C, Hötter AM, Muehlematter UJ, Burger IA, Donati OF, Barth BK. Value of bowel preparation techniques for prostate MRI: a preliminary study. *Abdom Radiol (NY)* 2021;46:4002-13.
 17. Roethke MC, Kuru TH, Radbruch A, Hadaschik B, Schlemmer HP. Prostate magnetic resonance imaging at 3 Tesla: Is administration of hyoscine-N-butyl-bromide mandatory? *World J Radiol* 2013;5:259-63.
 18. Vaughn BV, Rotolo S, Roth HL. Circadian rhythm and sleep influences on digestive physiology and disorders. *ChronoPhysiology and Therapy* 2014;4:67-77.
 19. Malone JC, Thavamani A. Physiology, Gastrocolic Reflex. In: StatPearls [Internet]. Treasure Island (FL): StatPearls Publishing; 2024. Available online: <https://www.ncbi.nlm.nih.gov/books/NBK549888/>
 20. Becker AS, Woo S, Leithner D, Tong A, Mayerhoefer ME, Vargas HA. The "Hungry Judge" effect on prostate MRI reporting: Chronobiological trends from 35'004 radiologist interpretations. *Eur J Radiol* 2024;179:111665.
 21. Caglic I, Hansen NL, Slough RA, Patterson AJ, Barrett T. Evaluating the effect of rectal distension on prostate multiparametric MRI image quality. *Eur J Radiol* 2017;90:174-80.
 22. Reischauer C, Cancelli T, Malekzadeh S, Froehlich JM, Thoeny HC. How to improve image quality of DWI of the prostate-enema or catheter preparation? *Eur Radiol* 2021;31:6708-16.
 23. Coskun M, Mehravand S, Shih JH, Merino MJ, Wood BJ, Pinto PA, Barrett T, Choyke PL, Turkbey B. Impact of bowel preparation with Fleet's™ enema on prostate MRI quality. *Abdom Radiol (NY)* 2020;45:4252-9.
 24. Padhani AR, Khoo VS, Suckling J, Husband JE, Leach MO, Dearnaley DP. Evaluating the effect of rectal distension and rectal movement on prostate gland position using cine MRI. *Int J Radiat Oncol Biol Phys* 1999;44:525-33.
 25. Dinkel J, Thieke C, Plathow C, Zamecnik P, Prüm H, Huber PE, Kauczor HU, Schlemmer HP, Zechmann CM. Respiratory-induced prostate motion: characterization and quantification in dynamic MRI. *Strahlenther Onkol* 2011;187:426-32.
 26. Hu L, Zhou DW, Guo XY, Xu WH, Wei LM, Zhao JG. Adversarial training for prostate cancer classification using magnetic resonance imaging. *Quant Imaging Med Surg* 2022;12:3276-87.
 27. Gao Z, Xu X, Sun H, Li T, Ding W, Duan Y, Tang L, Gu Y. The value of synthetic magnetic resonance imaging in the diagnosis and assessment of prostate cancer aggressiveness. *Quant Imaging Med Surg* 2024;14:5473-89.
 28. Sun Z, Wang K, Wu C, Chen Y, Kong Z, She L, Song B, Luo N, Wu P, Wang X, Zhang X, Wang X. Using an artificial intelligence model to detect and localize visible clinically significant prostate cancer in prostate magnetic resonance imaging: a multicenter external validation study. *Quant Imaging Med Surg* 2024;14:43-60.
 29. Mayer R, Simone CB 2nd, Turkbey B, Choyke P. Development and testing quantitative metrics from multiparametric magnetic resonance imaging that predict Gleason score for prostate tumors. *Quant Imaging Med Surg* 2022;12:1859-70.
 30. Qin X, Mu R, Zheng W, Li X, Liu F, Zhuang Z, Yang P, Zhu X. Comparison and combination of amide proton transfer magnetic resonance imaging and the apparent diffusion coefficient in differentiating the grades of prostate cancer. *Quant Imaging Med Surg* 2023;13:812-24.
 31. Li M, Ding N, Yin S, Lu Y, Ji Y, Jin L. Enhancing automatic prediction of clinically significant prostate cancer with deep transfer learning 2.5-dimensional segmentation on bi-parametric magnetic resonance imaging (bp-MRI). *Quant Imaging Med Surg* 2024;14:4893-902.
 32. Wagnerova M, Macova I, Hanus P, Jurka M, Capoun O, Lambert L, Burgetova A. Quantification and significance of extraprostatic findings on prostate MRI: a retrospective analysis and three-tier classification. *Insights Imaging* 2023;14:215.

Cite this article as: Lambert L, Macova I, Wagnerova M, Jurka M, Burgetova R, Capoun O, Burgetova A. The impact of modifiable factors on image quality of prostate magnetic resonance imaging and PI-RADS scores. *Quant Imaging Med Surg* 2025;15(3):2433-2443. doi: 10.21037/qims-24-1776